

Synthesis and Densification Behaviour of Bi-Based Superconducting Powder by Organic Precursor

A. Tampieri & G. Celotti

Research Institute for Ceramic Technology (IRTEC-CNR), via Granarolo 64, 48018 Faenza, Italy

(Received 4 July 1994; revised version received 7 February 1995; accepted 14 February 1995)

Abstract

BSCCO (2223) phase superconducting powder was synthesized by pyrolysis of a solution of citrates containing cations in the relative amounts required to prepare compounds with the nominal composition $\text{Bi}_{1.84}\text{Pb}_{0.35}\text{Sr}_{1.9}\text{Ca}_{2.1}\text{Cu}_3\text{O}_x$. Starting from the pyrolysed precursor, the preparation of (2 2 2 3) monophasic powder is realized in very short processing time of only 24 h. Reactions among components were investigated by thermogravimetric and differential thermal analysis; the products obtained on treating powders at various temperatures in the range 500–950°C were defined by XRD. The identification of the reaction intermediates that play a crucial role in the synthetic process was systematically performed, and a comparison with the solid-state reaction method was carried out. Hot pressing was performed in order to prepare highly dense superconducting materials. The densification behaviour of the powder obtained by the citrate route was studied in comparison with the solid-state reacted one.

1 Introduction

Several studies reported the existence of many difficulties in preparing Bi-based superconducting phases, mainly regarding the isolation of the high- T_c phase (2223) as a single phase. Indeed, incomplete reaction, compositional inhomogeneity, very large particle size and long sintering treatment are still typical trademarks of the conventional BSCCO solid-state synthesis. The use of the solution method to prepare organic precursor by pyrolysis overcomes these problems, producing highly homogeneous mixing with good stoichiometric control and constituted by active submicronic particles, characterized by a greater degree of reproducibility.^{1,2} It is already known³ that the pyrolysed precursors and classical mixture of oxides and carbonates, subjected to the same thermal treatments, run along different routes,

characterized by different kinetics and generating peculiar reaction intermediates in the two cases.

The present work examines the reactions involved when the pyrolysed precursors are thermally treated and discusses the fundamental role of the Bi–Ca phases as reaction intermediates highly affecting the superconducting phase synthesis rate. Evaluation of the densification behaviour and the sintering efficiency of the citrate powder compared to the solid-state reacted one, during hot pressing, has been performed. Microstructural and electrical characterization of dense materials, produced with the pyrolysed powder, were also carried out.

2 Experimental Procedure

The detailed procedure for powder preparation with a nominal composition $\text{Bi}_{1.84}\text{Pb}_{0.35}\text{Sr}_{1.9}\text{Ca}_{2.1}\text{Cu}_3\text{O}_x$ using a citrate method is reported elsewhere.¹ The obtained powder was calcined at 800°C for 6 h, then fired at 846°C for 5 h and at 858°C for 13 h, with three interposed grindings. The intermediate reaction products obtained after each step were determined by careful interpretation of XRD spectra.

Differential thermal analysis (DTA) and thermogravimetric analysis (TGA) were carried out on the pyrolysed mixture up to 1000°C. To investigate the DTA curve, various thermal treatments up to temperatures in the range 580–930°C were also performed and the products examined by XRD analysis using graphite monochromatized CuK_α radiation.

Morphology of powders and dense samples was investigated by means of Scanning Electron Microscopy (Leica Cambridge Ltd).

The obtained powders were hot-pressed in air using an alumina die with a pressure of 10 MPa; the sintering temperatures were 790 and 800°C and the sintering time under pressure was 2 h. Shrinkage was continuously recorded during sintering and the obtained density reported versus

time. Sample densities were measured by Archimedes' method. The degree of (001) texture orientation (Lotgering factor) in dense samples was also determined by XRD analysis. Electrical resistance of the dense samples was measured by means of the four-probe method with Ag paste contacts which were dried and hardened at 100°C for 10 min.

3 Results and Discussion

Micrograph in Fig. 1 shows spongy agglomerates as the product of the pyrolysis process, consisting of spherical submicronic primary particles (0.2–0.4 μm in diameter) connected to each other by necks partially sintered during the combustion process. Some of these agglomerates are rich in amorphous phases that, hardly detectable even by XRD, are revealed by thermoanalytical investigations.

In Fig. 2 the TG and DTA curves reveal that the precursor powder starts to react at about 500°C and the reaction develops via a complex process. The first step in the TG curve is attributed to the decomposition of $\text{Ca}_{0.33}\text{Pb}_{0.67}(\text{NO}_3)_2$, mainly present in the amorphous state (thus undetectable by XRD), followed by the decomposition of CaCO_3 , between 580 and 780°C, present with different degree of crystallinity.



Fig. 1. SEM micrograph of as-pyrolysed BSCCO powder.

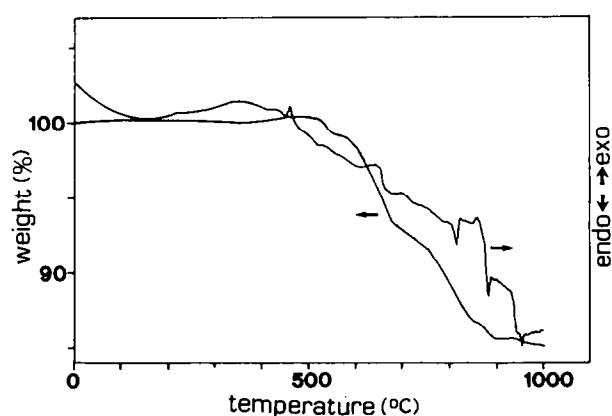


Fig. 2. Thermogravimetric and differential thermal analysis of pyrolysed powder.

The weight loss starting at 780°C is due to the beginning of SrCO_3 decomposition that runs out at $T \approx 930^\circ\text{C}$. The DTA peaks clearly evident during the thermal analysis of the carbonate and oxide mixing used as a precursor of the solid-state reaction procedure,^{4,5} are smoothed and broadened in the thermoanalytical curve of the pyrolysed precursor due to their low crystallinity. The DTA peaks between 630 and 730°C are attributable to various Bi–Ca phase formations and their interconversion from one form to another more stable one.⁶ At 730°C, the $\text{Bi}_6\text{Ca}_4\text{O}_{13}$ phase starts to form, in equilibrium with traces of $\text{Bi}_6(\text{Ca,Sr})_5\text{O}_{14}$; the DTA peak at 815°C is attributed to the transformation of the orthorhombic $\text{Bi}_6\text{Ca}_4\text{O}_{13}$ phase into monoclinic $\text{Bi}_6(\text{Ca,Sr})_5\text{O}_{14}$. As the decomposition of SrCO_3 advances at $T > 820^\circ\text{C}$, the CuO species is contemporarily engaged to form $(\text{Ca,Sr})\text{CuO}_2$. Taking into account that the methodology used to identify the phases at different temperatures permits only the detection of products of irreversible reactions, it is, however, possible to attribute to the various Ca–Bi phases, and mainly to the ‘ O_{14} ’ phase, a dominant role in the superconducting phase formation process.

Table 1 shows the phase evolution, determined by XRD, in the pyrolysed powder, during the various steps of the 24 h processing to obtain 98% pure (2223) phase, as far as the phases belonging to Bi–Sr–Ca–Cu–O system are concerned, the exact amounts of Ca_2PbO_4 and Ca_2CuO_3 cannot be specified, their scattering powders being unknown referred to $\alpha\text{-Al}_2\text{O}_3$ standard, but in any case the involved quantities are limited.

The high concentration of ‘ O_{13} ’ and especially of ‘ O_{14} ’ phases after the calcination treatment is a distinctive factor of the pyrolysed precursor synthetic process with respect to the conventional mixture of oxides and carbonates. The formation and dynamic equilibrium of the $\text{Bi}_6\text{Ca}_4\text{O}_{13}$ and $\text{Bi}_6(\text{Ca,Sr})_5\text{O}_{14}$ phases cause a retardation in (2212) formation; as a consequence, the phase concentration starts to increase substantially only after the first firing step at 858°C, while the solid-state reacted powder already after calcination exhibits over 80% of (2212) phase. The slackened (2212) formation involves a delay in its grain growth at the considered stage. Taking into account the (2223) formation mechanism proposed by Wang *et al.*,⁷ in which after a nucleation on the (2212) particle surface the (2223) growth process is controlled by diffusion, the accelerating effect of the smaller (2212) grain size, typical of calcined pyrolysed powder, becomes clear.

Moreover, the starting submicronic dimension of the pyrolysed precursor grains, promoting the

Table 1. XRD phase analysis of pyrolysed powders after various synthesis steps

	<i>As pyrolysed</i>	<i>Thermal treatment</i>			
		<i>Calcined</i>	<i>5 h/846°C</i>	<i>5 h/858°C</i>	<i>5+3 h/858°C</i>
CaCO ₃	X				
SrCO ₃	X				
CuO	X	XX			
Ca _{1-x} CuO ₂	XX				
Bi ₂ CuO ₄	XXX				
Bi ₂ SrO ₄	X				
Bi ₂ CaO ₄	X				
(Ca,Sr)CuO ₂			X	X	
Ca ₂ CuO ₃			X	X	X
Ca ₂ PbO ₄		XX	XX	XX	XX
Cu ₂ SrO ₃		XX			
Bi ₆ (Ca,Sr) ₅ O ₁₄		XXX			
Bi ₆ Ca ₄ O ₁₃		X			
2201			X	X	tr.
2212		X	XXX	XXX	X
2223			tr.	XX	XXX

Semi-quantitative scale of XRD intensity on a logarithmic base is employed: XXX = 10³, XX = 10², X = 10¹, tr = 10⁰.

solid-state diffusion process, stimulates the interfacial reactions responsible for any intermediate and/or final phase growth.⁷

Micrographs in Fig. 3(a,b) show morphology differences between the two completely reacted powders: the one obtained by organic precursor is characterized by reduced average dimension of

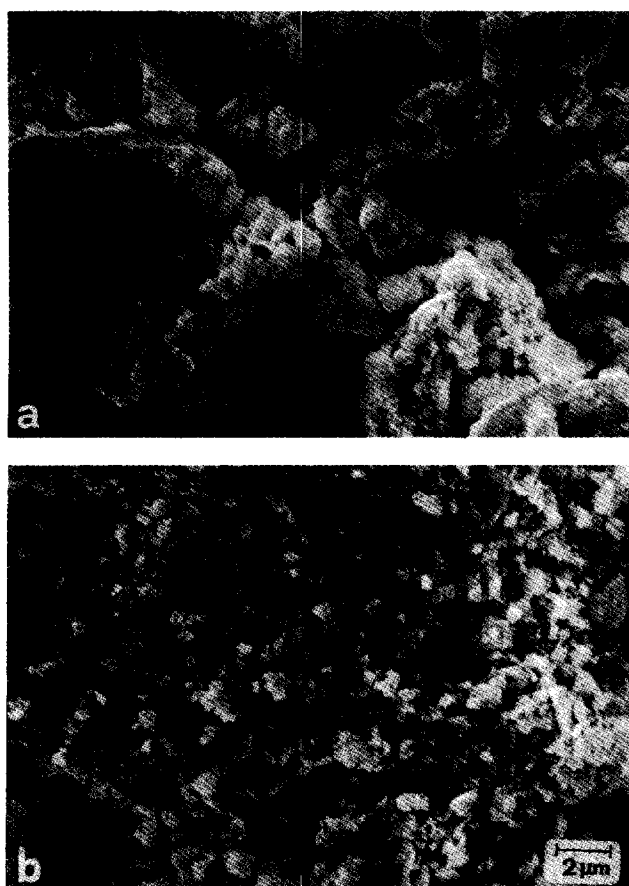


Fig. 3. SEM micrographs of BSCCO completely reacted powders ((2223) phase >95%): (a) solid state (96 h thermal treatment), (b) organic precursor (24 h thermal treatment).

grains (0.7 μm against 3.5 μm) and definitely less anisotropic shape. These features can explain the differences in green packing of the two powders: the powder by organic precursor shows significantly lower density values of green bodies compared to the solid-state reacted one. This reflects in the different starting points (time = 0) of the densification curves reported in Fig. 4, which shows the densification behaviour of the two powders during hot pressing at different temperatures.

It is evident that the densification rate increases with temperature and at 800°C the density value approach 100% after 2 h. The curves at 790°C were mathematically analysed on the basis of Brook's theory⁸ in order to establish the firing behaviour of the two powders in terms of the attainment of high density and the limitation of grain growth. Thus a parameter that relates the

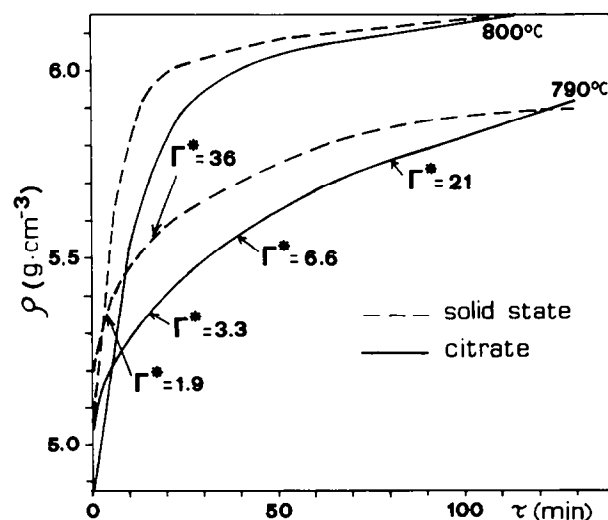


Fig. 4. Densification curves of solid-state reacted and citrate precursor powder; calculated figures of merit Γ^* are reported for some particular density values.

rate of grain growth and the densification rate is a figure of merit defined as:

$$\Gamma^* = -(1/3) \dot{\rho} \rho / \dot{\rho}^2$$

where $\dot{\rho}$ is the densification rate and $\dot{\rho}^*$ is the densification acceleration. The Γ^* values calculated at different densities along the densification curve (Fig. 4) evidence the behaviour of the two powders: the solid-state reacted powder, which starts the isothermal stage with better particles packing, densifies very rapidly up to 15 min and Γ^* is characterized by a low value, as expected for powders with high densification tendency (and low grain growth rate). At higher densities, Γ^* is lower for organic precursor powder, with respect to solid-state reacted one; in fact, the densification rate of the former increases, leading to the attainment of higher-density values over 120 min of hot-pressing treatment. Γ^* values also show that grain growth in the solid-state reacted powder (highly anisotropic in this case) is markedly enhanced (for densities higher than 80%), causing a reduction in the densification rate. Contemporarily, however, the more anisotropic grain growth allows the attainment of a higher degree of texture orientation (the orientation factor F in this case is $\approx 48\%$, to be compared with 35% for dense sample obtained by organic precursor powder). The citrate powder, characterized by a lower green packing, but able to achieve a higher density in long hot-pressing treatments, produces dense material with a low Lotgering factor, owing to the larger randomness in orientation of less anisotropically grown grains.

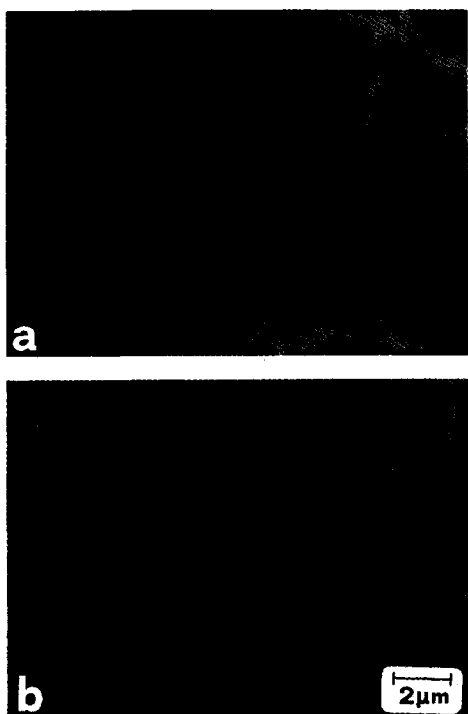


Fig. 5. SEM micrographs of fracture surfaces showing the morphology of hot-pressed dense samples obtained by (a) solid-state reacted powder, (b) citrate precursor powder.

Table 2. Properties of dense samples obtained by pyrolysed powder

Sample	Sintering temperature (°C)	RD (%)	F (%)	$T_{c \text{ onset}}$ (K)	$T_{c \text{ offset}}$ (K)
1	790	94	35	110	92
2	800	98	38	115	106

In Fig. 5(a,b) the morphology of hot-pressed samples is reported, showing the reduced average dimension of grains (about 2/5) of the sample prepared by organic precursors with respect to that obtained by solid-state reacted powder.

The properties of the hot-pressed samples are reported in Table 2. Critical temperature evaluated on dense samples showed $T_{c \text{ onset}}$ values ≈ 110 K, proving the substantial (2223) phase purity of the bulk.

The presence of a tailing phenomenon on Sample 1,^{9,10} lowering the $T_{c \text{ offset}}$ (Table 2), is attributed to the still incomplete densification in comparison with Sample 2 and to the low oxygen income during densification itself. Indeed, it is well known¹¹ that a scarce diffusion of oxygen into the inner part of the sample causes a lowering of T_{c0} in the (2223) phase: actually the critical temperature of Sample 2 (as densified) was for this second reason very low ($T_{c0} \approx 80$ K).

Since an oxygen decrease in formula stoichiometry, typical of highly dense materials, could be supposed on the basis of cell parameters evaluated by XRD analysis, Sample 2 was annealed at 820°C for 40 h in flowing air in order to restore the cell parameters themselves, and T_{c0} increased up to 106 K.

4 Conclusions

The citrate solution pyrolysis as an alternative method of preparing precursors for synthesis of BSCCO (2223) superconducting phase was performed and analysed, and inherent differences in comparison with traditional solid-state mixtures of oxides and carbonates were found: intermediate Bi–Ca phases play a determinant role in the organic precursor transformation, retarding the (2212) appearance and allowing the formation of (2223) phase in a total heat-treatment time at least four times shorter.

As expected, grain development is smaller for citrate precursor powder, and their shape is clearly more isotropic; densification exhibits a rather slow rate at the beginning, but within two hours powders by citrates reach and even exceed density values typical of solid-state reacted powders.

Critical temperatures result not too far from

those obtained with solid-state reacted powders, though lesser orientation factors attained by citrate precursor powders point to presumably lower transport current values; anyway, the probable compensating effects of different pinning centre concentrations deserve further investigation.

References

1. Tampieri, A., Celotti, G., Ricciardiello, F. & Russo, G., *Physica C*, **227** (1994) 300–8.
2. Sun, Y. K. & Lee, W. Y., *Physica C*, **212** (1993) 37–42.
3. Shimono, I., Nagata, S., Konishi, H. & Hamaguchi, Y., *Jpn. J. Ceram. Soc.*, **101** (1993) 1018–24.
4. Tampieri, A., Landi, E. & Bellosi, A., *Mater. Chem. and Phys.*, **34** (1993) 157–61.
5. Lo, W., Chen, Y. L., Tang, T. B. & Stevens, R., *Br. Ceram. Trans. J.*, **89** (1990) 218–22.
6. Boehnke, U. C., Heitman, P., Krötzsch, M., Lippold, B. & Zahn, G., *J. Mater. Sci.*, **28** (1993) 111–6.
7. Wang, M., Xiong, G., Tang, X. & Hong, Z., *Physica C*, **210** (1993) 413–6.
8. Pickup, H., Gilbert, E., Brook, R. J., Leriche, A. & Cambier, F., *Proc. 2nd Int. Symp. on Ceramic Materials and Components for Engines*, Lübeck, 14–17 April, 1986, pp. 63–70.
9. Murayama, N., Kodama, Y., Sakaguchi, S. & Wakai, F., *Jpn. J. Ceram. Soc.*, **100** (1992) 236–9.
10. Celotti, G., Tampieri, A., Masini, R. & Malpezzi, M. C., *Physica C*, **225** (1994) 346–52.
11. Nomura, S., Yoshino, H. & Ando, K., *J. Am. Ceram. Soc.*, **76** (1993) 2687–90.